Environmental Science & Technology

Article

pubs.acs.org/est

Depassivation of Aged Fe^0 by Divalent Cations: Correlation between Contaminant Degradation and Surface Complexation Constants

Tongxu Liu,[†,‡] Xiaomin Li,[‡] and T. David Waite*[,‡]

[†]Guangdong Key Lab. of Agricultural Environment Pollution Integrated Control, Guangdong Institute of Eco-Environmental and Soil Sciences, Guangzhou 510650, People's Republic of China

[‡]School of Civil and Environmental Engineering, University of New South Wales, Sydney, New South Wales 2052, Australia

Supporting Information

ABSTRACT: The dechlorination of trichloroethylene (TCE) by aged Fe^0 in the presence of a series of divalent cations was investigated with the result that while no significant degradation of TCE was observed in Milli-Q water or in solutions of Ba^{2+}, Sr^{2+}, or Ca^{2+}, very effective TCE removal was observed in solutions containing Mg^{2+}, Mn^{2+}, Co^{2+}, Fe^{2+}, Ni^{2+}, Zn^{2+}, Cu^{2+}, or Pb^{2+}. The rate constants of TCE removal in the presence of particular cations were positively correlated to the log *K* representing the affinity of the cations for hydrous ferric oxide (HFO) surface sites though the treatments with Co^{2+} and Ni^{2+} were found to provide particularly strong enhancement in TCE degradation rate. The extent of Fe(II) release to solution also increased with increase in log *K*, while the solution pH from both experimental measurement and thermodynamic calculation decreased with increasing log *K*. While the peak areas of Fe and O XPS spectra of the passivated ZVI in the presence of Ba^{2+}, Sr^{2+}, and Ca^{2+} were very close to those in Milli-Q water, very significant increases in surface Fe and O (and OH) were observed in solutions of Mg^{2+}, Mn^{2+}, Co^{2+}, Fe^{2+}, Ni^{2+}, Zn^{2+}, Cu^{2+} and Pb^{2+}, revealing that the surface oxide layer dissolution is consistent with the recovery of aged Fe^0 with respect to TCE degradation. The depassivation process is proposed to involve (i) surface complexation of cations on surface coatings of aged Fe^0, (ii) dissolution of the hydrated surface as a consequence of magnetite exposure, and (iii) transport of electrons from underlying Fe^0 via magnetite to TCE, resulting in TCE dechlorination and, for some cations (Co^{2+}, Ni^{2+}, Cu^{2+}, and Pb^{2+}), reduction to their zero or +1 valence state (with potential for these reduced metals to enhance TCE degradation).

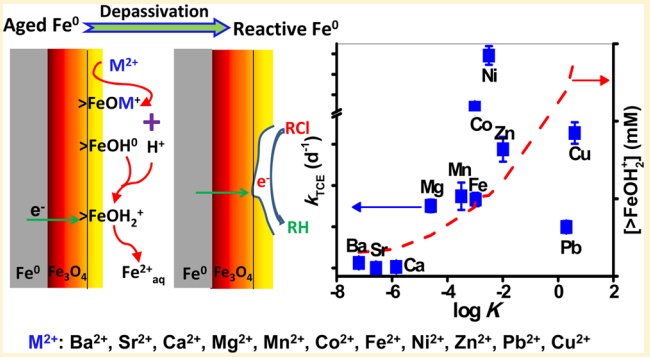

INTRODUCTION

Zerovalent iron (ZVI, Fe^0) can degrade or transform a wide range of reducible contaminants with the result that permeable reactive barriers of Fe^0 have been successfully applied for the remediation of contaminated groundwater.[1−3] However, many studies have shown that aging (or longevity) is one of the most important and potentially limiting factors in the use of Fe^0 to reduce groundwater contaminants.[4,5] Storage of Fe^0 particles and their exposure to the atmosphere results in a significant decrease in their reactivity with time because the reactive Fe^0 sites become covered with Fe(III) oxides with these surface coatings reducing the efficiency of electron transfer from Fe^0 to the contaminant.[6,7] As such, the passivation of reactive Fe^0 is of major concern as it severely limits the practical application of ZVI technology.

A number of approaches have been developed to recover or sustain the reactivity of aged Fe^0, including dissolution of iron oxide coatings using an improved flash-drying protocol after acid washing[8] and application of strong reductants such as dithionite and borohydride to reduce Fe(III) minerals to the active zerovalent state or ferrous form.[9,10] The emplacement of organic surface coating on ZVI has also attracted considerable attention in view of the ability of these coatings to both minimize formation of oxide coatings and prevent aggregation and sedimentation of the particles.[11] However, these methods involve a pretreatment step that adds complexity and cost to the ZVI technology and, if at all possible, would be best avoided.

It has been reported that some components of natural waters (or wastewaters) may induce the depassivation of aged Fe^0 thereby minimizing the cost and complexity of pretreatment.[12−16] Indeed, we recently reported that Mg^{2+} ions, at concentrations typical of that in seawater, can depassivate aged Fe^0 as a result of promotion of surface dissolution arising from proton release during formation of the $>FeOMg^+$ surface complex and, as a result, can enhance trichloroethylene (TCE) degradation by aged Fe^0.[17] We also found that Fe^{2+} ions, which may be present at relatively high concentrations in anoxic pore waters as a result of the reductive dissolution of Fe(III) oxyhydroxides, could similarly induce the depassivation of aged

Received: August 3, 2014
Revised: October 24, 2014
Accepted: November 10, 2014
Published: November 10, 2014

Fe^0 and, as a result, significantly enhance the rate of reduction of contaminants in contact with aged Fe^0.[18]

The findings described above raise the question of generality of the ability of divalent cations which sorb to the iron oxyhydroxide coatings on Fe^0 to depassivate the aged zerovalent iron, particularly as a wide range of these cations may be present in subsurface environments affected by, for example, acid mine drainage,[19] flue gas desulfurization (FGD) wastewater and electroplating wastewaters.[20] While few relevant studies have been reported, Doong and Lai[21] provide evidence that some transition metals (Co^{2+}, Ni^{2+}, and Cu^{2+}) enhance the rate of dechlorination of TCE and PCE by Fe^0 though for these redox active metals, an enhancement mechanism related more to their ability to be reduced to their zerovalent state with resultant increased reducing capacity of the composite system rather than any effect related to surface complex formation and acid-induced destabilization of the passivating iron oxyhydroxide coatings was proposed.

In view of the above discussion, it is apparent that we are unable as yet to propose a general mechanism for the impact of divalent metals on the reductive ability of aged (passivated) Fe^0. As such, the aim of this study is (i) to confirm whether the presence of particular cations including alkaline metals (e.g., Ba^{2+} and Sr^{2+}), transition metals (e.g., Mn^{2+}, Co^{2+}, Ni^{2+}, Zn^{2+}, and Cu^{2+}), and other metals (e.g., Pb^{2+}) affect the reactivity of aged Fe^0 via possible depassivation in a manner similar to Mg^{2+} and Fe^{2+}, (ii) to correlate the observed reactivity of aged Fe^0 with the properties of any cation(s) present, and (iii) to provide a general understanding of the influence of cations on depassivation of aged Fe^0 such that it will be possible to predict the reducing ability of aged Fe^0 in any particular situation where the composition of the liquid phase in contact with the passivated particles is known.

EXPERIMENTAL SECTION

Materials. Zerovalent iron (Fe^0, powder, ~70 mesh, 99%) was obtained from Acros Organics (Product No. 197815000) and was kept in the sealed bottle in which it was delivered for around three months before it was opened and used. After opening, the iron powder was stored in air for around one year prior to use. Preliminary experiments indicated minimal change in reactivity after this aging time though, for consistency, any set of studies was undertaken on material that had been aged for the same period.[4] The average particle size was measured (using a Malvern Mastersizer 2000C) to be around 167 μm. The material was principally Fe^0 but with traces of oxides (Fe_3O_4 and FeO) present as a surface layer.[18] Trichloroethylene (TCE, 99+%), $MgCl_2{\cdot}6H_2O$ (99%), $CaCl_2$ (99+%), $SrCl_2{\cdot}6H_2O$ (99%), $BaCl_2{\cdot}2H_2O$ (99%), $MnCl_2{\cdot}4H_2O$ (98%), $CoCl_2{\cdot}6H_2O$ (99+%), $FeCl_2{\cdot}4H_2O$ (99%), $NiCl_2$ (99%), $ZnCl_2$ (99%), $CuCl_2$ (99%), and $PbCl_2$ (99%) were obtained from Sigma-Aldrich in Australia. All solutions were prepared in Milli-Q water. High-performance liquid chromatography (HPLC)-grade methanol and *n*-hexane (Sigma-Aldrich) were used without further purification.

Experimental Procedure. The aged Fe^0 (1 g) was preweighed in each test serum bottle (120 mL) with the serum bottles then filled with 40 mL of either Milli-Q water (as control), or solutions of individual salts (10 mM) as follows: $MgCl_2$, $CaCl_2$, $SrCl_2$, $BaCl_2$, $MnCl_2$, $CoCl_2$, $FeCl_2$, $NiCl_2$, $ZnCl_2$, $CuCl_2$, and $PbCl_2$. (Note that these concentrations of Ca^{2+} and Mg^{2+} are typical of those found in seawater while heavy metals concentrations of 10 mM or more are common in effluents discharged from industries such as electroplating, mining and battery manufacturing.)[22,23] The Milli-Q water and stock solutions of salts were purged with O_2-free argon gas for more than 2 h before being transferred to an anaerobic chamber in which standard anaerobic techniques were used in the following experimental procedure. TCE in the methanol stock solution was added to the reaction solution at a final concentration of 0.22 mM before the serum bottles were sealed with Teflon-coated butyl rubber stoppers and crimp seals. All studies were conducted in duplicate with vials incubated in a shaker at 200 rpm at 25 °C. Sampling intervals were arranged on days 1, 3, 5, 7, 10, 14, and 21.

Analytical Methods. Samples (0.15 mL) were extracted with 1.5 mL *n*-hexane for TCE determination, which was carried out using a gas chromatograph (Agilent 6890) equipped with an ECD detector and Trace TR-5MS silica fused capillary column (30 m × 0.25 mm i.d., 0.25 μm film thickness). The injector temperature was 250 °C and the helium flow rate was 1.0 mL min^{-1}. The column temperature was set at 100 °C for 2 min and increased at a rate of 15 °C min^{-1} to 160 °C, then switched to a rate of 5 °C min^{-1}. The temperature was finally increased to 250 °C and maintained isothermally for 10 min. TCE external standards were prepared in *n*-hexane with standard curves found to be linear. The average of duplicate determinations of concentration is reported with relative percent differences found to be typically less than 10%. As TCE is volatile and partitions between the liquid and gas phases, the total moles of TCE remaining in both liquid and gas phases were calculated using a Henry's Law constant for TCE of 0.009 37 atm m^3 mol^{-1} (the proportion of moles of TCE in the liquid phase was typically on the order of 0.54).

For determination of dissolved Fe(II) concentrations, the samples were centrifuged at 1000*g* for 5 min at 25 °C and the supernatant filtered using a 0.22-μm syringe filter before analysis. Dissolved Fe(II) was measured colorimetrically by the 1,10-phenathroline colorimetric method. All manipulations related to preparing the samples for Fe(II) determination by 1,10-phenathroline were conducted inside the anaerobic chamber prior to colorimetric measurement. The amounts of Fe(II) sorbing to the syringe filter used in measuring these concentrations can be ignored based on calibration curves of Fe(II) standards developed with and without the use of syringe filters.

To determine the crystal phase composition of the samples after 21 days' incubation, the reaction suspensions were centrifuged at 1000*g* for 5 min, and the precipitation was then dried for 48 h by freeze-dry methods. X-ray diffraction (XRD) measurement was carried out at room temperature using an X'Pert PRO Muti-purpose X-ray Diffraction System (MPD system) with Cu Kα radiation (λ = 0.154 18 nm). The phases were identified by comparing diffraction patterns with those on the standard powder XRD cards compiled by the Joint Committee on Powder Diffraction Standards (JCPDS). An accelerating voltage of 45 kV and emission current of 40 mA were used. Surface analysis of ZVI was performed with an XPS (ESCALAB250Xi, Thermo Scientific, U.K.). The X-ray source was a monochromated Al K alpha (energy 1486.68 eV) with the X-ray beam monochromatized using seven crystals mounted on three Rowland circles. The energy was analyzed using a high-resolution 200 mm mean radius hemispherical electrostatic analyzer and detected by a multichannel plate-CCD camera. The pass energy was 100 eV for survey scans or 20 eV for region scans. Binding energies of the photoelectrons were correlated to the adventitious hydrocarbon C(1s) peak at 285.0 eV.

Table 1. Parameters for ZVI and Hydrous Ferric Oxide (HFO, 1 g L^{-1}, 600 m^2 g^{-1}) Suspension in the Presence of Different Cations (10 mM)

	25 g L^{-1} Fe^0 (measured)			1 g L^{-1} HFO (calculated)			
cations	k (d^{-1})	dissolved Fe(II) (mM)	pH	log K	>$FeOH_2^+$ (mM)	>$FeOM^+$ (mM)	pH
Milli-Q	0.00 ± 0.00	0.00 ± 0.00	10.9 ± 0.1		0.26		7.5
Ba^{2+}	0.01 ± 0.01	0.00 ± 0.00	10.0 ± 0.1	−7.20	0.26	0.00	7.4
Sr^{2+}	0.00 ± 0.00	0.00 ± 0.00	10.2 ± 0.3	−6.58	0.27	0.01	7.4
Ca^{2+}	0.00 ± 0.00	0.00 ± 0.03	10.6 ± 0.2	−5.85	0.27	0.03	7.2
Mg^{2+}	0.15 ± 0.02	0.11 ± 0.01	8.5 ± 0.3	−4.60	0.31	0.11	6.9
Mn^{2+}	0.17 ± 0.03	0.32 ± 0.08	7.9 ± 0.3	−3.50	0.36	0.14	6.3
Co^{2+}	0.72 ± 0.03	3.95 ± 0.30	7.4 ± 0.3	−3.01	0.38	0.18	6.1
Fe^{2+}	0.17 ± 0.02	6.87 ± 0.36	7.8 ± 0.1	−2.98	0.40	0.16	6.1
Ni^{2+}	5.85 ± 0.91	6.75 ± 0.78	7.4 ± 0.1	−2.50	0.41	0.23	5.9
Zn^{2+}	0.29 ± 0.03	10.99 ± 0.79	7.1 ± 0.2	−1.99	0.45	0.27	5.7
Pb^{2+}	0.10 ± 0.01	6.52 ± 0.45	6.6 ± 0.4	0.30	0.68	0.61	4.7
Cu^{2+}	0.33 ± 0.03	7.16 ± 0.50	7.3 ± 0.2	0.60	0.76	0.72	4.4

Equilibrium speciation of salt ions and surface complexes was carried out using the thermodynamic package Visual MINTEQ 3.0. While the systems under investigation here were not at equilibrium in all aspects, speciation modeling was restricted to conditions where an iron oxyhydroxide surface coating was present on the Fe^0 surface and pseudoequilibrium for major ions and iron species could be reasonably assumed.[18]

RESULTS AND DISCUSSION

TCE Reduction by Aged Fe^0 in the Presence of Various Cations. Kinetics of TCE degradation by aged Fe^0 in solutions with 11 different cation salts in Milli-Q water are shown in Supporting Information (SI) Figure S1 as are the results of control studies showing no TCE degradation in salt solutions in the absence of Fe^0. No significant degradation of TCE by aged Fe^0 was observed in Milli-Q water or in the solutions of $BaCl_2$, $SrCl_2$, and $CaCl_2$. As previously reported,[17] the presence of low concentrations of Cl^- (<50 mM) had little influence on TCE degradation by aged Fe^0 with these results suggesting that aged Fe^0 cannot be activated by the cations Ba^{2+}, Sr^{2+}, and Ca^{2+}. Very effective TCE removal by aged Fe^0 was observed in solutions of $MgCl_2$, $MnCl_2$, $CoCl_2$, $FeCl_2$, $NiCl_2$, $ZnCl_2$, $PbCl_2$, and $CuCl_2$, indicating that aged Fe^0 can be activated by the cations Mg^{2+}, Mn^{2+}, Co^{2+}, Fe^{2+}, Ni^{2+}, Zn^{2+}, Cu^{2+} and Pb^{2+}. The pseudo-first-order rate constants (k) are summarized in Table 1. While the k values in the presence of cations Ba^{2+}, Sr^{2+}, and Ca^{2+} (≤0.013 d^{-1}) were close to the control without any added cations, the k values in the presence of the other cations (0.099 d^{-1} − 5.853 d^{-1}) were much higher than those induced by the presence of Ba^{2+}, Sr^{2+}, or Ca^{2+}. The first order rate constants (k) for TCE degradation by aged Fe^0 in the presence of most cations (Mg^{2+}, Mn^{2+}, Fe^{2+}, Zn^{2+}, Pb^{2+}, and Cu^{2+}) fell in a relatively narrow range (0.099−0.327 d^{-1}), but the value was somewhat higher in the presence of Co^{2+} (0.724 d^{-1}) and dramatically higher in the presence of Ni^{2+} (5.853 d^{-1}). While we have not conducted an investigation of the concentration dependence of all the cations examined here, results of our previous studies[17,18] showed that the depassivation effects were very dependent on cation concentration with effects evident but much weaker at concentrations 2 orders of magnitude lower than used here.

Effects of Cations on the Solution pH and Fe(II). To examine whether changes in acidity occurred as a result of either salt hydrolysis or surface complexation processes, pH values after 21 days of reaction were measured. (The initial pH of Milli-Q is ~7.0, which increases to 10.5 after adding ZVI, and then decreases to different pH as indicated in Table 1 after adding cations). Results in Table 1 indicate that the final pH values in the Fe^0 suspension with $BaCl_2$, $SrCl_2$, and $CaCl_2$ were close to that without any added cations (10.9), while the pH values decreased to 6.5−8.5 in the presence of $MgCl_2$, $MnCl_2$, $CoCl_2$, $FeCl_2$, $NiCl_2$, $ZnCl_2$, $PbCl_2$, and $CuCl_2$. Results of dissolved Fe(II) analyses are shown in Table 1 and indicate that less than 0.002 mM of dissolved Fe(II) was detected in the treatments with $BaCl_2$, $SrCl_2$, and $CaCl_2$, while an obvious increase in dissolved Fe(II) from 0.11 mM to 10.99 mM was found in the presence of $MgCl_2$, $MnCl_2$, $CoCl_2$, $FeCl_2$, $NiCl_2$, $ZnCl_2$, $PbCl_2$, and $CuCl_2$. This pH decrease and Fe(II) release were presumably associated with proton (H^+) release in the presence of cations with proton release possibly inducing dissolution of the passivating film on the aged Fe^0 surface with concomitant release of dissolved iron into solution.[17,18]

Correlation between the Reactivity of Aged Fe^0 and Surface Complexation Constants. It has been reported elsewhere that an iron oxyhydroxide surface coating is present on the Fe^0 surface and pseudoequilibrium for major ions with this iron oxyhydroxide coating can be reasonably assumed.[24] Interaction of cations with hydroxylated sites on the iron oxyhydroxide surface (>$FeOH^0$) will involve formation of cation-oxygen bonds and can be represented by the "surface complexation" reaction shown in eq 1:

$$M^{2+} + >FeOH^0 \rightleftharpoons >FeOM(II)^+ + H^+ \quad (1)$$

where M^{2+} represents a divalent cation (i.e., Ba^{2+}, Sr^{2+}, Ca^{2+}, Mg^{2+}, Mn^{2+}, Co^{2+}, Fe^{2+}, Ni^{2+}, Zn^{2+}, Cu^{2+}, or Pb^{2+}).

Previous studies[18] revealed that formation of >$FeOFe(II)^+$ is critical to the extent of proton release in the presence of added Fe^{2+} with the associated decrease in solution pH inducing an increase in concentration of the surface species >$FeOH_2^+$, with the rate of dissolution of iron oxides considered to be proportional to the concentration of this relatively labile species.[25] In accord with this mechanism, Liu et al.[17] suggested that the dissolution processes can be described by the reactions shown in eqs 2 and 3:

$$>FeOH^0 + H^+ \rightleftharpoons >FeOH_2^+ \quad (2)$$

$$Fe^0 + 2>FeOH_2^+ + 4H^+ \rightarrow 3Fe^{2+} + 4H_2O \quad (3)$$

Release of Fe^{2+} ions will leave "fresh" Fe^0 and >$FeOH_2^+$ sites until both the underlying zerovalent iron particle and the passivating iron oxyhydroxide surface layer are consumed. In light of this

dx.doi.org/10.1021/es503777a | Environ. Sci. Technol. 2014, 48, 14564−14571

proposed mechanism, the extent of formation of $>FeOH_2^+$ in the presence of surface reactive cations would be expected to be determined by the extent of proton release on formation of the surface complex (eq 1) with those complexes exhibiting higher stability constants (K) expected to result in greater proton release (for any given cation concentration), greater decrease in pH and greater lability of surface sites. The log K values for the complexes formed between the various cations and iron oxyhydroxide surface sites are given in Table 1 and are ranked as $Ba^{2+} < Sr^{2+} < Ca^{2+} < Mg^{2+} < Mn^{2+} < Co^{2+} < Fe^{2+} < Ni^{2+} < Zn^{2+} < Pb^{2+} < Cu^{2+}$. The rate constants ($k$), measured pH and dissolved Fe(II) are plotted as a function of log K in Figure 1. The plot of k vs log K (Figure 1a) suggests that the k values of most cations are positively correlated to the log K values of the surface complex formed between the cations and iron oxyhydroxide surface sites. Some anomalies are evident with the k value for Co^{2+} (0.724 d^{-1}) more than four times that of Fe^{2+} (0.174 d^{-1}) or Mn^{2+} (0.166 d^{-1}) despite the surface complexes for these cations exhibiting very similar log K values. Even more dramatically, the k value for Ni^{2+} (5.853 d^{-1}) is more than 20 times that for Zn^{2+} (0.288 d^{-1}) even though the log K values for the surface complexes of these metals are very similar. However, the k value for Pb^{2+} (0.099 d^{-1}) is lower than that for Mg^{2+}, Mn^{2+}, Co^{2+}, Fe^{2+}, Ni^{2+}, Zn^{2+}, and Cu^{2+} even though their log K values are all lower than that of Pb^{2+}. In spite of the exceptions for Co^{2+}, Ni^{2+}, and Pb^{2+}, the results strongly confirm the positive correlation of TCE degradation rate constant with the log K values of the surface complexes formed between the cations and iron oxyhydroxide surface sites.

The plot of measured pH vs log K shown in Figure 1b suggests that while the final pH for ZVI in Milli-Q water was 10.89, the final pH in the presence of cations decreased gradually from the highest pH (10–10.5 for Ba^{2+}, Sr^{2+}, and Ca^{2+}) to lowest pH (~6.5 for Pb^{2+}) with increasing log K value. In addition, the final dissolved Fe(II) concentration shown in Figure 1c increased slightly from ~0 mM (Ba^{2+} and Sr^{2+}) to 0.322 mM (Mn^{2+}) and then increased sharply to 3.95–10.99 mM (Co^{2+}, Fe^{2+}, Ni^{2+}, and Zn^{2+}). Even though lower values were observed for Cu^{2+} and Pb^{2+} than might have been expected from the $[Fe^{2+}]$ versus log K behavior for the other cations, it would appear reasonable to conclude that the extent of surface dissolution was strongly influenced by the log K values of the surface complexes for the various cations. The correlation of the TCE degradation rate, final pH and dissolved Fe(II) concentration with the log K of the cation surface complex (except in cases where elemental forms of the cations were most likely present) are further illustrated in SI Figure S2.

The concentrations of the $>FeOH_2^+$ and $>FeOM(II)^+$ surface species as well as the solution pH calculated using Visual MINTEQ assuming the initial presence of 10 mM of the different cation salts (or Milli-Q water as comparison) with the surface of aged Fe^0 assumed to be covered by HFO (1 g L^{-1}, 600 m^2 g^{-1}) are shown in Table 1 and plotted against the log K values for surface complexes of the various cations in Figure 2. The concentrations of $>FeOH_2^+$ and $>FeOM(II)^+$ increased gradually with increasing log K values while the calculated pH decreased gradually. While both the measured and calculated pH values exhibited a decrease with increasing log K values, the measured pH values were significantly higher than the calculated pH values. For example, the initial pH of HFO without any cation was calculated to be 7.45, while the initial pH of aged Fe^0 suspension in the absence of any added cation was measured to

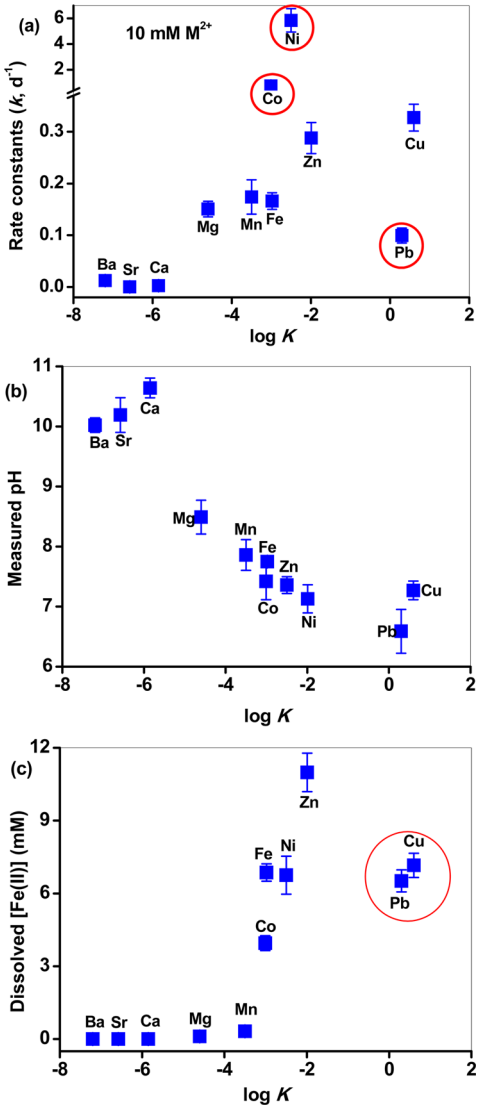

Figure 1. Correlation of (a) the pseudo-first order rate constants (k) of TCE degradation, (b) the final pH, and (c) dissolved Fe(II) with log K values of different cations on hydrous ferric oxide (HFO, 1 g L^{-1}, 600 m^2 g^{-1}). The final pH and dissolved Fe(II) were measured after 21 days' reaction in serum bottles.

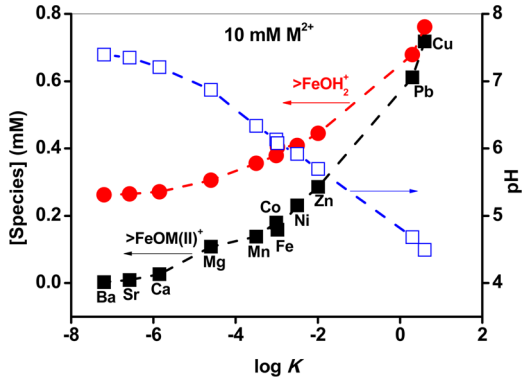

Figure 2. Correlation of model predicted results for $>FeOH_2^+$, $>FeOM(II)^+$, and calculated pH in suspension of HFO (1 g L^{-1}, 600 m^2 g^{-1}) containing different cations (10 mM) with log K values of different cations on HFO.

dx.doi.org/10.1021/es503777a | Environ. Sci. Technol. 2014, 48, 14564–14571

be 10.89. A possible reason for the discrepancy between measured and calculated initial pH is a lack of accounting for effects of hydration of surface oxide coatings in our thermodynamic modeling (see SI Table S1 and associated description). To investigate this possibility, the time dependent change in pH of suspensions resulting from addition of appropriate amounts of ferrihydrite, goethite, hematite, magnetite, and wüstite was measured with results shown in SI Figure S3. The results indicate that while there were no obvious changes in pH (~7.2) of the suspensions containing ferrihydrite, goethite, hematite, and magnetite, the pH of the wüstite suspension increased slightly from 7.3 to ~8.0.

Another reason for the observed rapid initial increase in pH on addition of passivated Fe^0 to aqueous solutions may be related to the possible presence of defects (including pits, pinholes and cracks) in the passivating film as suggested[4,26,27] with these defects enabling reaction of H_2O with underlying Fe^0 with resultant production of OH^- ions (i.e., $Fe^0 + 2H_2O \rightarrow Fe^{2+} + 2OH^- + H_2$). This reaction would be expected to be relatively short-lived as the Fe^{2+} generated by this reaction will quickly precipitate as fresh ferrous oxide or hydroxide passivating materials (i.e., FeO or $Fe(OH)_2$). The rapidity with which any exposed Fe^0 is passivated may the reason for the lack of any evidence of reduction of TCE in these systems. The fact that no Fe^0 is evident in these passivated materials by XPS indicates that the Fe^0 remains well below the surface (if indeed the presence of defects in the dry passivating layer is the reason for the rapid initial pH increase on exposure of these materials to aqueous solution).

No TCE degradation was observed in the presence of cation alone (i.e., in the absence of aged Fe^0), suggesting that the solution phase species cannot contribute directly to TCE degradation. However, the results in SI Table S1 and Figure S4 show that a correlation of the log K values of the dominant aqueous species (MOH^+) with rates of TCE degradation (SI Figure S4a), or Fe(II) formation (SI Figure S4b) is evident. While we would not expect that the MOH^+ is directly related to the depassivation process, the tendency to form the MOH^+ species might be indirectly related to depassivation behavior of the cation (i.e., the stronger the tendency to form MOH^+, the greater the extent of proton release and thus the greater the tendency to dissolve the iron oxide passivating layer). Furthermore, the solution pH is directly related to the tendency to form MOH^+ as proton release accompanies the formation of these hydroxylated species ($M^{2+} + H_2O = MOH^+ + H^+$). Results in SI Figure S4c show that the measured pH was well correlated with the log K of MOH^+, suggesting that the overall measured pH decrease was also influenced by the formation of MOH^+. According to the results in Figure 1b and SI Figure S4c, both MOH^+ and $>FeOM^+$ contributed to the pH decrease in the system of aged Fe^0 and cation.

Chemical State of Aged Fe^0 Surface after Reaction with Cations. The release of dissolved Fe(II) to solution confirms that the presence of cations results in the destruction of the passivating iron oxide layer on the surface of aged Fe^0 with Fe(II) being formed as a result of either oxidative dissolution of the underlying Fe^0 and/or (Fe^0-mediated) reductive dissolution of the Fe(III) oxide passivating layer.[18] XRD analysis of the Fe^0 particles after 21 days' reaction with TCE in the presence of the various added cations showed similar patterns in most cases to the system to which no cations had been added (SI Figure S5) with Fe^0 and Fe_3O_4 identified as the major components present and with weak FeO signals, indicating its presence as a minor crystal phase. However, peaks of Fe_3O_4 increased significantly in the presence of Cu^{2+}, presumably because the presence of Cu^{2+} enhanced the Fe(II)-catalyzed transformation from amorphous iron oxyhydroxide to magnetite,[28] and two new peaks at 31.2° and 36.2° were also observed in the presence of Pb^{2+}, with these peaks attributable to the formation of Pb^0 on the surface.[29,30]

While the presence or absence of amorphous iron oxyhydroxide coatings on the Fe^0 would not be detectable by XRD, XPS can be used to characterize the chemical state of surface elements. Since XPS is a truly surface analysis technique with less than 10 nm probing depth, the Fe^0 peak at a binding energy (BE) of ~707 eV was not discernible in the XPS spectrum of any of our samples (Figure 3a). The Fe 2p spectra consists of a 2p3/2 peak

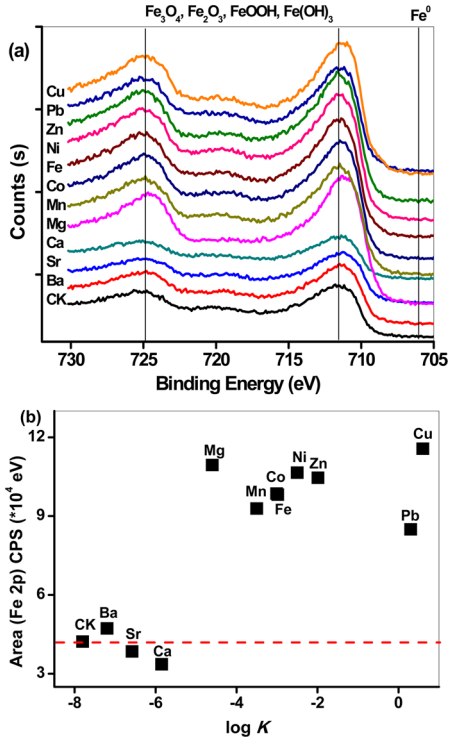

Figure 3. (a) XPS Fe 2p region spectra of aged Fe^0 (25 g L^{-1}) in solutions of 10 mM of various cations after reaction with TCE for 21 days, and (b) Correlation of peak areas of decomposed peaks with log K values of different cations on HFO. The area of Fe 2p was determined from the peaks in the range of 706−739 eV.

at a binding energy (BE) of ~711 eV and a 2p1/2 peak at a BE of ~725 eV in BE with these peaks representative of the presence of iron oxides/hydroxides.[31] While results in Figure 3b show that the areas of these peaks in the presence of cations Ba^{2+}, Sr^{2+}, and Ca^{2+} (i.e., those with low log K values (≤ -5.85)) were similar to those for aged ZVI in the absence of any added cations, the areas of these peaks increased significantly with increasing log K values for the cations with log $K \geq -4.60$ (i.e., Mg^{2+}, Mn^{2+}, Co^{2+}, Fe^{2+}, Ni^{2+}, Zn^{2+}, Pb^{2+}, and Cu^{2+}) with this increase presumably related to an increase in the extent of oxide formation on reaction of passivated ZVI with these cations. This result is supported by the effect of the presence of cations on the area of the O 1s photoelectron peak (SI Figure S6a) with this area also reflective of the nature and extent of surface oxide coatings.[5,32,33] As can be seen in SI Figure S6b, the total area of the O 1s peak increased slightly following reaction of aged ZVI in solutions containing Ba^{2+}, Sr^{2+}, or Ca^{2+} (i.e., the cations with low log K values) but

dx.doi.org/10.1021/es503777a | Environ. Sci. Technol. 2014, 48, 14564−14571

increased markedly in the presence of the cations with log $K \geq -4.60$ (i.e., Mg^{2+}, Mn^{2+}, Co^{2+}, Fe^{2+}, Ni^{2+}, Zn^{2+}, Pb^{2+}, and Cu^{2+}). This increase can again be ascribed to the increased oxide proportion present following reaction of aged ZVI with cations with surface oxide formed by precipitation of iron oxides following dissolution of passivating iron oxide layers and, in some instances, precipitation of an oxide of the added cation (with this latter process likely to occur for Mn^{2+}, Pb^{2+}, and Cu^{2+}). On the basis of the above discussion, it can be concluded that the presence of cations with high log K values indeed destroyed passivating surface layers on the aged Fe^0 with the presence of these cations leading to a higher density of surface oxygen species via the surface dissolution and reprecipitation of iron oxides and, in some instances, the accumulation of cation oxides.

In addition, a "step-like behavior" is apparent in Figures 1 and 3, where it appears that some type of threshold must be met before significant dissolution of the passivating layer, decrease in pH and degradation of the contaminant is observed. Specifically, it appears that the strength of interaction of Ba, Sr, and Ca with the iron oxyhydroxide passivating layer is too weak to induce significant dissolution, with dissolution and resulting pH decrease and contaminant degradation only apparent for elements that interact more strongly with the FeOOH passivating layer. For log $K > -6$, we observe a generally ordered increase in dissolution rate, decrease in pH, and release of Fe(II) as log K increases, although some elements (particularly Ni and Pb) induce atypical behavior for reasons discussed as below (such as formation of zeo valent elements on exposure to the underlying Fe^0).

Chemical State of the Cations on Aged Fe^0 Surface. The XPS spectra of the cations on the ZVI surface are shown in SI Figure S7 with these spectra showing that the valence state of most of the cation metals on the mZVI surface remains unchanged on reaction with ZVI. For example, the XPS spectra exhibit the peaks for Ba^{2+} (780.6 eV), Sr^{2+} (134.2 eV), Ca^{2+} (347.9 eV), Mg^{2+} (1304.4 eV), and Zn^{2+} (1022.4 eV), respectively, confirming that the valence states of these metals are Ba(II), Sr(II), Ca(II), Mg(II), and Zn(II), respectively.[31,34,35] As such, these metals react with the ZVI surface via adsorption or surface complexation with no change in the metal valence; an observation in accord with the standard oxidation−reduction potentials of these metal ions compared to that of Fe^0.[25] As shown in SI Table S2, metals such as Ba^0, Sr^0, Ca^0, Mg^0, and Zn^0 have E^0 values that are more negative than that of Fe^0 and, as such, reduction of the metal ions by Fe^0 is not expected occur on the ZVI surface with any surface reaction involving sorption/surface complexation only. For metals with an E^0 value far more positive than that of Fe^0 (such as Co^0, Ni^0, Cu^0, and Pb^0), cation reduction via electron transfer from Fe^0 was thermodynamically feasible. However, only a few cations were found to be present in their reduced state with most either remaining unchanged or present in mixed valence states. For example, peaks at 932 eV can be attributed to the presence of Cu(0), peaks at 932.9 eV to the presence of Cu(I) and peaks at 934.9 eV representative of the presence of Cu(II). The observation of peaks at 852.1 and 855.5 eV indicate that both Ni(0) and Ni(II) are present on the ZVI surface. Similarly, in solutions containing the lead salt, peaks indicative if the presence of Pb(0) (at 136.4 eV) and Pb(I) (at 138.0 eV) were evident and, in solutions containing cobalt, peaks indicative of the presence of Co(0) (at 780 eV) and Co(II) (at 797.6 eV) were evident. Importantly, the zerovalent forms of elements other than iron are recognized to have strong reductive dechlorination capacity and can be assumed to contribute to TCE degradation in the aged Fe^0 system. In addition, the reduced forms of some cations, including Co(I),[36] Cu(I),[37] Mn(II),[38] and Fe(II),[18] have been shown to exhibit the capacity for reductive degradation of chlorinated compounds and may well contribute to the degradation of TCE in the studies described here.

Mechanisms of Cation-Mediated Depassivation of Aged Fe^0. On the basis of the results presented both above and in our earlier work,[17,18] we conclude that the complexation of cations on the oxide coatings of aged Fe^0 is critical to removal of the oxide coating with initial association between the cation and surface hydroxyl groups resulting in proton release and decrease in pH with the depassivated ZVI then capable of inducing contaminant reduction until all consumed. This decrease in pH is associated with an increase in proportion of the surface species $>FeOH_2^+$ with the rate of dissolution of metal oxides shown to be directly proportional to the concentration of this fully protonated surface species[39] (as is evident from Table 1 and Figures 1 and 2). As the metal ion released to solution was in the form of Fe(II), reduction of Fe(III) present in the relatively unstable $>FeOH_2^+$ species was presumably induced by reaction with underlying Fe^0. In addition, the concentration of $>FeOH_2^+$ predicted to form was heavily dependent on the log K of the surface complex $>FeOM(II)^+$ presumed to form at surface sites of the iron oxide passivating layer, suggesting that the rate and extent of dissolution of surface oxide coatings is also determined by the surface complexation constants (log K). Results of TCE degradation, final pH, and dissolved Fe(II) concentration confirmed that the cation-induced depassivation behavior of aged Fe^0, once a threshold binding strength had been exceeded, was reasonably correlated with the log K of the cation surface complex (except in cases where elemental forms of the cations were most likely present).

For Fe^{2+} addition, the surface complex $>FeOFe(II)^+$ is a potential reductant but has been shown to have limited capacity for TCE dechlorination.[18] For the other cations, the surface complex $>FeOM(II)^+$ may, in some instances, contribute to the TCE dechlorination. While the reductive dechlorination of organic chlorinated compounds has not been reported for the surface-sorbed Ba^{2+}, Sr^{2+}, Ca^{2+} Mg^{2+}, Mn^{2+}, Ni^{2+}, Zn^{2+}, and Pb^{2+}), surface-sorbed Co^{2+} has been shown to be capable of PCE and TCE dechlorination and hence may play a role in the aged ZVI/Co system investigated here. Since some cations (particularly Cu^{2+}, Co^{2+}, Ni^{2+}, and Pb^{2+}) will be reduced if they come in contact with the underlying Fe^0,[36−38] the resultant reduced forms of those cations may also influence the overall TCE degradation. In this regard, Li and Zhang[31] have previously shown that Ni^{2+}, following its reduction to Ni^0 by underlying Fe^0, is very effective in reducing TCE both via direct reduction and via its role as an electron sink in enhancing TCE reduction by Fe^0. For Co^{2+}, the possible intermediate product ($>FeOCo(I)^0$) has been shown to be capable of PCE and TCE dechlorination[36] and hence is a possible reductant of TCE in the ZVI-Co^{2+} system. As shown by Doong and Lai,[25] Co^0 also has the capacity for TCE degradation. For Cu^{2+}, the reduced products ($>FeOCu(I)^0$ and Cu^0) formed via reduction of Cu^{2+} by underlying Fe^0, have the capacity for TCE reduction.[40,41] Similarly, Pb^{2+} can be reduced to Pb^0 by underlying Fe^0 with the bimetallic Fe—Pb shown to be effective for TCE dechlorination.[29,30]

Depassivation of aged Fe^0 by metals such as Ni^{2+} and Co^{2+} is recognized to occur as a result of the reduction of those cations to species which are either able to reduce TCE or to act as electron sinks which can catalyze TCE reduction. However, no real

correlation is evident (or, indeed, expected) between TCE degradation rate constants and the E^0 of the various cations (SI Figure S8), as most cations remain in their divalent state. Therefore, this explanation cannot account for the recognized ability of other cations which cannot be reduced by Fe^0, such as Mg^{2+}, Mn^{2+}, and Zn^{2+}, to depassivate aged Fe^0 (as revealed here by their induction of rapid TCE degradation). This indicates that the first step of cation-induced depassivation of aged Fe^0 is most likely related to the dissolution of passivating iron oxide surface layers that occurs as a result of cation adsorption and subsequent proton release with some cations (Co^{2+}, Ni^{2+}, and Cu^{2+}) further enhancing TCE reduction as a result of the reduction of the contaminant by zero or single valent species. In addition, the reduction of TCE by zero or single valent species (in systems where such species can be formed) is likely to be the dominant process with dissolution of the oxyhydroxide coating layer in these cases a minor contributor to the overall degradation process.

With regard to the electron transfer process from underlying Fe^0 to redox active surface species such as Co^{2+}, Ni^{2+}, and Cu^{2+}, Li and Zhang[24,31] proposed that the iron oxide shell can be considered as an n-type semiconductor with the conduction band (CB) of those iron oxide materials mediating the electron transfer from the underlying Fe^0 to the surface sorbed electron acceptors. In this case, TCE adsorbed on the surface should also be reduced by these CB electrons of iron oxide coatings (SI Table S2 and associated description), however no significant TCE degradation was observed in the system of aged Fe^0 with Milli-Q water, indicating either that TCE cannot trap the electron from the CB or that no electrons were transferred from the underlying Fe^0 via the outer oxide layer. It has been reported in many studies[5,6,24,27] that the outer surface layer is composed of amorphous iron oxyhydroxide or goethite or lepidocrocite, which may block the electron transfer from Fe^0 to surface. The XPS results also show that the outer surface is covered by >OH or $>OH_2$ groups with these surface entities overlying magnetite and wüstite (based on the XRD results). The results reported here suggest that the cations can induce the dissolution of surface outer layers with resultant exposure of magnetite, a conducting iron oxide phase which has the capacity of transferring electrons from the underlying Fe^0.

In summary, the divalent cation-induced depassivation process proposed here is presented in Figure 4 and involves (i) surface complexation of cations on surface coatings of aged Fe^0, (ii) dissolution of the hydrated surface iron oxide coating with exposure of the underlying magnetite, and (iii) electron transfer from the underlying Fe^0 via magnetite to TCE followed by TCE dechlorination. Additionally, redox active cations (Co^{2+}, Ni^{2+}, Cu^{2+}, and Pb^{2+}) can be reduced to zero or single valent species with the potential capacity of TCE degradation. The rate of removal of the passivating iron oxyhydroxide layer would appear to be dependent on the affinity of the cation for iron oxyhydroxide surface sites with the time taken for coating removal presumably dependent on both this affinity and the thickness of the layer. More rapid reduction of contaminants occurs in instances where zerovalent forms of the cation are generated.

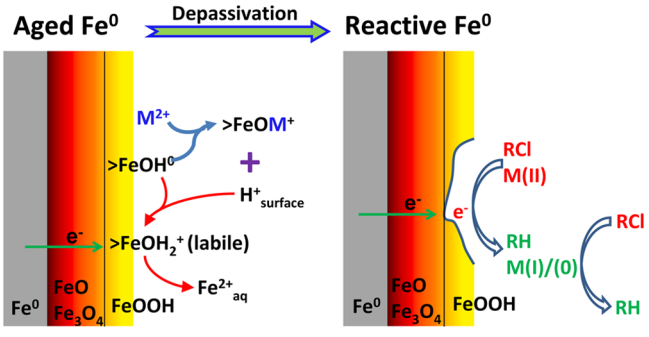

Figure 4. Schematic illustrations of the cation-induced depassivation process of aged Fe^0. The left represents the aged Fe^0, and the right one represents the reactive Fe^0 after surface dissolution by cations. M^{2+}: Ba^{2+}, Sr^{2+}, Ca^{2+}, Mg^{2+}, Mn^{2+}, Co^{2+}, Fe^{2+}, Ni^{2+}, Zn^{2+}, Pb^{2+}, and Cu^{2+}.

It is well recognized that fresh Fe^0 is usually used immediately after synthesized in contaminant degradation experiments. However, when exposed to air, it readily reacts with oxygen and water vapor in the air with resultant formation of oxide or hydroxide coatings which prevent electron flow from the underlying Fe^0 to surface located contaminants.[4] In our current study, the commercial Fe^0 did not show any capacity for TCE degradation, while very effective degradation of this contaminant was observed in solutions containing particular divalent cations. From an applications perspective, our findings show that aged Fe^0 can be used directly for contaminant removal provided "corrosive" cations (such as Mg, Mn, Fe, Zn, and Co) are present.

■ ASSOCIATED CONTENT

Ⓢ Supporting Information

Kinetics of TCE transformation by aged Fe^0 in the solution with individual inorganic salts, XRD patterns of Fe^0 particles after reaction with cations and TCE reduction, XPS spectra of individual cations and all the O 1s, and summary of the surface complexation constants, pH, surface species, dissolved Fe(II) and rate constants. This material is available free of charge via the Internet at http://pubs.acs.org.

■ AUTHOR INFORMATION

Corresponding Author

*Phone: +61-2-9385 5060; e-mail: d.waite@unsw.edu.au.

Notes

The authors declare no competing financial interest.

■ ACKNOWLEDGMENTS

T.X.L. acknowledges the award of a UNSW Vice-Chancellor's Post-Doctoral Research Fellowship with Supplementary Research Support Grant (No. RG114816). The authors also acknowledge support provided through ARC Linkage Project LP100100852.

■ REFERENCES

(1) Johnson, T. L.; Scherer, M. M.; Tratnyek, P. G. Kinetics of halogenated organic compound degradation by iron metal. *Environ. Sci. Technol.* **1996**, *30*, 2634−2640.

(2) Lackovic, J. A.; Nikolaidis, N. P.; Dobbs, G. M. Inorganic arsenic removal by zero-valent iron. *Environ. Eng. Sci.* **2000**, *17*, 29−39.

(3) Li, L.; Fan, M. H.; Brown, R. C.; Wang, J. J.; Wang, W. H.; Song, Y. H.; Zhang, P. Y. Synthesis, properties and environmental applications of nanoscale iron-based materials: A review. *Crit. Rev. Environ. Sci. Technol.* **2006**, *36*, 405−431.

(4) Sarathy, V.; Tratnyek, P. G.; Nurmi, J. T.; Baer, D. R.; Amonette, J. E.; Chun, C.; Penn, R. L.; Reardon, E. J. Aging of iron nanoparticles in aqueous solution: Effects on structure and reactivity. *J. Phys. Chem. C* **2008**, *112*, 2286−2293.

(5) Wang, C.; Baer, D. R.; Amonette, J. E.; Engelhard, M. H.; Antony, J.; Qiang, Y. Morphology and electronic structure of the oxide shell on

the surface of iron nanoparticles. *J. Am. Chem. Soc.* **2009**, *131*, 8824−8832.
(6) Kim, H. S.; Ahn, J. Y.; Hwang, K. Y.; Kim, I. K.; Hwang, I. Atmospherically stable nanoscale zero-valent iron particles formed under controlled air Contact: Characteristics and reactivity. *Environ. Sci. Technol.* **2010**, *44*, 1760−1766.
(7) Phillips, D. H.; Gu, B.; Watson, D. B.; Roh, Y.; Liang, L.; Lee, S. Y. Performance evaluation of a zerovalent iron reactive barrier: Mineralogical characteristics. *Environ. Sci. Technol.* **2000**, *34*, 4169−4176.
(8) Nurmi, J. T.; Sarathy, V.; Tratnyek, P. G.; Baer, D. R.; Amonette, J. E.; Karkamkar, A. Recovery of iron/iron oxide nanoparticles from solution: comparison of methods and their effects. *J. Nanopart. Res.* **2011**, *13*, 1937−1952.
(9) Zhu, B. W.; Lim, T. T. Catalytic reduction of chlorobenzenes with Pd/Fe nanoparticles: Reactive sites, catalyst stability, particle aging, and regeneration. *Environ. Sci. Technol.* **2007**, *41*, 7523−7529.
(10) Xie, Y.; Cwiertny, D. M. Use of dithionite to extend the reactive lifetime of nanoscale zero-valent iron treatment systems. *Environ. Sci. Technol.* **2010**, *44*, 8649−8655.
(11) Tratnyek, P. G.; Salter-Blanc, A. J.; Nurmi, J. T.; Amonette, J. E.; Liu, J.; Wang, C. M. Dohnalkova, A.; Baer, D. R. Reactivity of Zerovalent Metals in Aquatic Media: Effects of Organic Surface Coatings. In Tratnyek, P., et al. *Aquatic Redox Chemistry* **2011**, Chapter *18*, 381−406.
(12) Shih, Y.; Chen, M. Y.; Su, Y. F. Pentachlorophenol reduction by Pd/Fe bimetallic nanoparticles: Effects of copper, nickel, and ferric cations. *Appl. Catal. B: Environ.* **2011**, *105*, 24−29.
(13) Shih, Y.; Chen, M. Y.; Su, Y. F. Pentachlorophenol reduction by Pd/Fe bimetallic nanoparticles: Effects of copper, nickel, and ferric cations. *Appl. Catal., B* **2011**, *105*, 24−29.
(14) Chun, C. L.; Baer, D. R.; Matson, D. W.; Amonette, J. E.; Penn, R. L. Characterization and reactivity of iron nanoparticles prepared with added Cu, Pd, and Ni. *Environ. Sci. Technol.* **2010**, *44*, 5079−5085.
(15) Lien, H. L.; Jhuo, Y. S.; Chen, L. H. Effect of heavy metals on dechlorination of carbon tetrachloride by iron nanoparticles. *Environ. Eng. Sci.* **2007**, *24*, 21−30.
(16) Schrick, B.; Blough, J. L.; Jones, A. D.; Mallouk, T. E. Hydrodechlorination of trichloroethylene to hydrocarbons using bimetallic nickel-iron nanoparticles. *Chem. Mater.* **2002**, *14*, 5140−5147.
(17) Liu, T. X.; Li, X. M.; Waite, T. D. Depassivation of aged Fe^0 by inorganic salts: Implications to contaminant degradation in seawater. *Environ. Sci. Technol.* **2013**, *47*, 7350−7356.
(18) Liu, T. X.; Li, X. M.; Waite, T. D. Depassivation of aged Fe^0 by ferrous ions: Implications to contaminant degradation. *Environ. Sci. Technol.* **2013**, *47*, 13712−13720.
(19) Wilkin, R. T.; McNeil, M. S. Laboratory evaluation of zero-valent iron to treat water impacted by acid mine drainage. *Chemosphere* **2003**, *53*, 715−725.
(20) Huang, Y. H.; Peddi, P. K.; Tang, C.; Zeng, H. Hybrid zero-valent iron process for removing heavy metals and nitrate from flue-gas-desulfurization wastewater. *Sep. Purif. Technol.* **2013**, *118*, 690−698.
(21) Doong, R.; Lai, Y. Effect of metal ions and humic acid on the dechlorination of tetrachloroethylene by zerovalent iron. *Chemosphere* **2006**, *64*, 371−378.
(22) Revathi, M.; Saravanan, M.; Chiya, A. B.; Velan, M. Removal of copper, nickel, and zinc ions from electroplating rinse water. *Clean − Soil, Air, Water* **2012**, *40*, 66−79.
(23) Tang, C.; Huang, Y. H.; Zeng, H.; Zhang, Z. Promotion effect of Mn^{2+} and Co^{2+} on selenate reduction by zero-valent iron. *Chem. Eng. J.* **2014**, *244*, 97−104.
(24) Li, X. Q.; Zhang, W. X. Iron nanoparticles: The core-shell structure and unique properties for Ni(II) sequestration. *Langmuir* **2006**, *22*, 4638−4642.
(25) Stumm, W.; Morgan, J. J. *Aquatic Chemistry, Chemical Equilibria and Rates in Natural Waters*, Third ed.; John Wiley & Sons, Inc.: New York, 1996; pp 489−491.
(26) Gaspar, D. J.; Lea, A. S.; Engelhard, M. H.; Baer, D. R.; Miehr, R.; Tratnyek, P. G. Evidence for localization of reaction upon reduction of carbon tetrachloride by granular iron. *Langmuir* **2002**, *18*, 7688−7693.
(27) Scherer, M. M.; Balko, B. A.; Tratnyek, P. G. The role of oxides in reduction reactions at the metal-water interface. In Mineral−Water Interfacial Reactions: Kinetics and Mechanisms; Sparks, D. L., Grundl, T. J., Eds.; American Chemical Society: Washington, DC, 1998; ACS Symposium Series, Vol. *715*, pp 301−322.
(28) Ishikawa, T.; Minamigawa, M.; Kandori, K.; Nakayama, T.; Tsubota, T. Influence of metal ions on the transformation of γ-FeOOH into α-FeOOH. *J. Electrochem. Soc.* **2004**, *151*, B512−B518.
(29) Nie, X.; Liu, J.; Yue, D.; Zeng, X.; Nie, Y. Dechlorination of hexachlorobenzene using lead-iron bimetallic particles. *Chemosphere* **2013**, *90*, 2403−2407.
(30) Niu, S.; Liu, Y.; Xu, X.; Lou, Z. Remediation of Cr(VI) and Pb(II) aqueous solutions using supported, nanoscale zero-valent iron. *Environ. Sci. Technol.* **2000**, *34*, 2564−2569.
(31) Li, X. Q.; Zhang, W. X. Sequestration of metal cations with zerovalent iron nanoparticles—A study with high resolution X-ray photoelectron spectroscopy (HR-XPS). *J. Phys. Chem. C* **2007**, *111*, 6939−6946.
(32) Signorini, L.; Pasquini, L.; Savini, L.; Carboni, R.; Boscherini, F.; Bonetti, E. Size-dependent oxidation in iron/iron oxide core-shell nanoparticles. *Phys. Rev. B* **2003**, *68*, 195423.
(33) Nurmi, J. T.; Tratnyek, P. G.; Sarathy, V.; Bear, D. R.; Amonette, J. E.; Peacher, K.; Wang, C.; Linehan, J. C.; Matson, D. W.; Penn, R. L.; Driessen, M. D. Characterization and properties of metallic iron nanoparticles: spectroscopy, electrochemistry, and kinetics. *Environ. Sci. Technol.* **2005**, *39*, 1221−1230.
(34) Norman, C.; Leach, C. In situ high temperature X-ray photoelectron spectroscopy study of barium strontium iron cobalt oxide. *J. Membr. Sci.* **2011**, *382*, 158−165.
(35) Woo, S. I.; Kim, J. S.; Jun, H. K. Characterization of Ca—Bi—Mo oxide catalyst for selective propane ammoxidation, using XRD, XPS, TPRX/TPRO, and IR/Raman. *J. Phys. Chem. B* **2004**, *108*, 8941−8946.
(36) Kliegman, S.; McNeill, K. Dechlorination of chloroethylenes by cob(I)alamin and cobalamin model complexes. *Dalton Trans.* **2008**, 4191−4201.
(37) Maithreepala, R. A.; Doong, R. A. Synergistic effect of copper ion on the reductive dechlorination of carbon tetrachloride by surface-bound Fe(II) associated with goethite. *Environ. Sci. Technol.* **2004**, *38*, 260−268.
(38) Biesinger, M. C.; Payne, B. P.; Grosvenor, A. P.; Lau, L. W. M.; Gerson, A. R.; Smart, R. St. C. Resolving surface chemical states in XPS analysis of first row transition metals, oxides and hydroxides: Cr, Mn, Fe, Co and Ni. *Appl. Surf. Sci.* **2011**, *257*, 2717−2730.
(39) Zinder, B.; Furrer, G.; Stumm, W. The coordination chemistry of weathering: II. Dissolution of Fe(III) oxides. *Geochim. Cosmochim. Acta* **1986**, *50*, 1861−1869.
(40) Maithreepala, R. A.; Doong, R. A. Reductive dechlorination of carbon tetrachloride in aqueous solutions containing ferrous and copper ions. *Environ. Sci. Technol.* **2004**, *38*, 6676−6684.
(41) Maithreepala, R. A.; Doong, R. A. Enhanced dechlorination of chlorinated methanes and ethenes by chloride green rust in the presence of copper(II). *Environ. Sci. Technol.* **2005**, *39*, 4082−4090.